



SEMI-ANALYTICAL STUDY OF FREE VIBRATION OF COMPOSITE SHELLS OF REVOLUTION BASED ON THE REISSNER-MINDLIN ASSUMPTION

Z. C. XI, L. H. YAM and T. P. LEUNG

Department of Mechanical and Marine Engineering, The Hong Kong Polytechnic University,
 Hung Hom, Kowloon, Hong Kong

(Received 26 May 1994)

Abstract A semi-analytical procedure is presented for predicting free vibration characteristics of composite shells of revolution. The approach considers both transverse shear deformation and the coupling between symmetric and unsymmetric modes in laminated composite shells. Numerical examples are given for the free vibrations of thin cylindrical laminated composite shells and moderately thick symmetric cross-ply and antisymmetric angle-ply laminated composite conical shells. The effects of shear deformation, circumferential wave number, thickness to radius ratio, ply angle and stacking sequence on natural frequency are discussed.

NOTATION

E, E_1, E_2	Young's modulus
$G, G_{12}, G_{23}, G_{13}$	shear modulus
h	thickness of shell wall
L	length of the meridian of the element
n	circumferential wave number
N_s, N_θ	element shape function defined as $N_s = 1 - \eta$ and $N_\theta = \eta$ with $\eta = s/L$
r	average radius of conical shell
R_1, R_2	radius of the cone at its small and large ends, respectively
s, θ, z	meridional, circumferential and radial coordinates, respectively
u, v, w	displacements in meridional, circumferential and radial directions, respectively
$\dot{u}, \dot{v}, \dot{w}$	velocities
β_s, β_θ	rotations of the normal to midplane around the s and θ axes, respectively
ν, ν_{12}	Poisson's ratio
ρ	mass density of material
ϕ	semi-vertex angle of the cone
ω	circular frequency
\mathbf{a}	vector of nodal displacements
$\ddot{\mathbf{a}}$	vector of nodal accelerations
$\mathbf{A}, \mathbf{B}, \mathbf{D}, \mathbf{A}_s$	matrices of extensional, extensional-bending coupling, bending and transverse shear stiffness for the laminated shell
$\bar{\mathbf{A}}, \bar{\mathbf{A}}_s$	defined by eqns (14) and (15), respectively
$\mathbf{C}^1, \mathbf{C}^2$	defined by eqn (17)
\mathbf{K}	stiffness matrix for the element
\mathbf{M}	mass matrix for the element
\mathbf{N}	matrix of shape functions for the element
$\bar{\mathbf{M}}$	vector of stress couples
$\bar{\mathbf{N}}$	vector of stress resultants
\mathbf{Q}	matrix of reduced stiffnesses for the ply
$\bar{\mathbf{Q}}$	matrix of transformed reduced stiffnesses for the ply
\mathbf{S}	vector of shear forces
$\boldsymbol{\gamma}$	vector of transverse shear strains
$\boldsymbol{\epsilon}$	vector of midplane strains
$\boldsymbol{\chi}$	vector of changes in the midsurface curvatures and twist
$\theta_s^0, \theta_\theta^0$	defined by eqns (8) and (9), respectively

1. INTRODUCTION

The semi-analytical procedure based on separating the variables in a Fourier series along the circumferential direction and using conical finite elements along the meridional direction

was first put forward by Grafton and Strome (1963). Later, considerable work was done to improve, develop and apply this process (Zienkiewicz and Taylor, 1989). The literature on the subject was well reviewed by Gallagher (1975). It is unnecessary to go into details here. The processes have been shown to be capable of reducing computational labour greatly if they are used to deal with the problem of isotropic axisymmetric shells.

The application of fibre-reinforced composite materials to the aerospace industry has promoted investigation of free vibration of laminated composite shells of revolution (Bert and Kumar, 1982; Noor and Burton, 1990; Bismarck-Nasr, 1992). Due to the limitation of the scope of this study, only the literature on semi-analytical studies of this problem is reviewed here.

A two-node straight truncated conical element was first formulated and was applied to the free vibration of axisymmetric orthotropic shells by Grafton and Strome (1963). A 16 degrees of freedom element based on high-order shape functions was developed and was used to study the axisymmetric vibration of laminated shells by Shivakumar and Krisnamurthy (1978). An unaxisymmetric truncated conical element considering the displacement in the circumferential direction was presented and was employed to deal with laminated composite shells of revolution by Sheinman and Grief (1984). The vibration analysis of orthotropic cantilever cylindrical shells with axial thickness variation was carried out by Sivadas and Ganesan (1992). It should be pointed out emphatically that, unlike isotropic shells, laminated composite shells are anisotropic and non-homogeneous. They possess strong extensional-shear, extensional-bending and bending-twisting coupling effects. Even if both shells and loadings are axisymmetric, vibrations of shells still involve symmetric and antisymmetric modes. In other words, symmetric and antisymmetric vibrations of composite shells are coupled with each other. Because the above-mentioned references do not consider this coupling effect, they are applicable only to isotropic, orthotropic and cross-ply shells of revolution. In the context of semi-analytical analysis, only Sheinman and Weissman (1987) considered the coupling between symmetric and antisymmetric modes in composite shells of revolution by using the unaxisymmetric conical element based on the Kirchhoff-Love assumption.

Most of the advanced composites in use to date have a low ratio of the transverse shear modulus to the in-plane modulus. Application of thick composite shells of revolution in industries has also been increasing. These shells exhibit strong transverse shear deformation effects. However, few researchers have presented a semi-analytical method considering both transverse shear deformation and the coupling between symmetric and antisymmetric modes.

The main objective of this paper, therefore, is to develop a semi-analytical procedure for considering both transverse shear deformation and the coupling between symmetric and unsymmetric modes for predicting free vibration characteristics of laminated composite shells of revolution. Numerical examples are given for free vibrations of thin laminated composite cylindrical shells and thick symmetric cross-ply and antisymmetric angle-ply laminated composite conical shells. The effects of shear deformation, wave number, thickness to radius ratio, ply angle and stacking sequence on natural frequency are discussed.

2. FORMULATION

The Reissner-Mindlin postulates are adopted to consider transverse shear deformation. In principle, these assumptions are for thick shells, but they are applicable to both thick and thin shells by using reduced integration (Zienkiewicz and Taylor, 1989). Consider a laminated composite conical shell shown in Fig. 1. Let ϕ and r denote the semi-vertex angle and average radius of the cone, respectively. The coordinate system $s\theta z$ is adopted. u , v and w are the displacements in the meridional, circumferential and radial directions, respectively; β_s and β_θ are the rotations of the normal to the midplane around the s and θ axes, respectively. Using the Reissner-Mindlin assumptions, the eight strain components

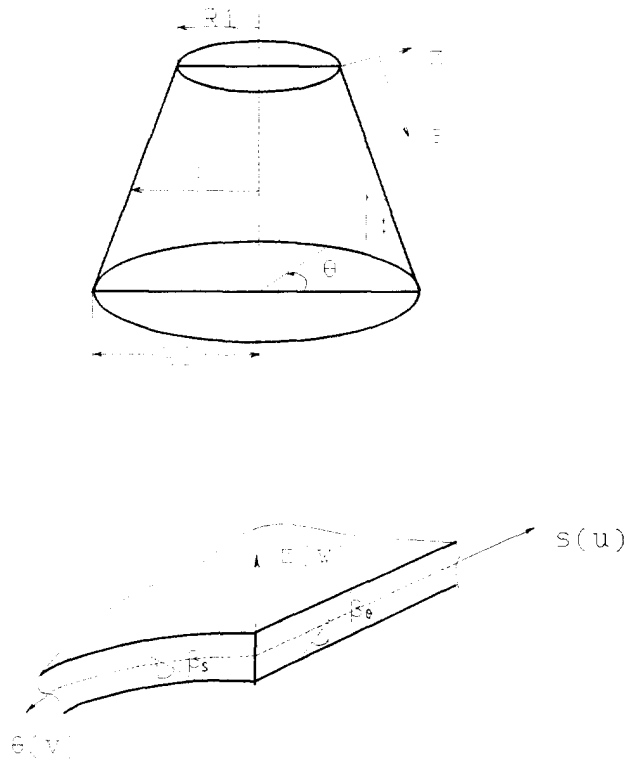


Fig. 1. Definitions of variables for shell approximation.

are given by the following expression (Cook, 1981):

$$\mathbf{e} = \begin{Bmatrix} e_{11} \\ e_{22} \\ e_{33} \\ e_{12} \\ e_{13} \\ e_{23} \end{Bmatrix} = \begin{Bmatrix} \frac{\partial u}{\partial s} \\ \frac{1}{r} \left(\frac{\partial r}{\partial \theta} + u \sin \phi + w \cos \phi \right) \\ \frac{\partial v}{\partial s} - \frac{1}{r} \left(\frac{\partial u}{\partial \theta} - v \sin \phi \right) \\ \frac{\partial u}{\partial s} \\ \frac{\partial v}{\partial s} \\ \frac{\partial w}{\partial s} \end{Bmatrix} \quad (1)$$

$$\mathbf{\chi} = \begin{Bmatrix} \chi_1 \\ \chi_2 \\ \chi_3 \end{Bmatrix} = \begin{Bmatrix} \frac{\partial \beta_s}{\partial s} \\ -\frac{1}{r} \frac{\partial \beta_\theta}{\partial \theta} - \frac{\sin \phi}{r} \beta_\theta \\ \frac{1}{r} \frac{\partial \beta_\theta}{\partial \theta} - \frac{\partial \beta_s}{\partial s} + \frac{\sin \phi}{r} \beta_s - \frac{\cos \phi}{2r} \left(\frac{\partial u}{\partial \theta} - \frac{\partial v}{\partial s} - \frac{\sin \phi}{r} v \right) \end{Bmatrix} \quad (2)$$

$$\mathbf{\gamma} = \begin{Bmatrix} \gamma_1 \\ \gamma_2 \end{Bmatrix} = \begin{Bmatrix} \frac{1}{r} \frac{\partial w}{\partial \theta} - \frac{\cos \phi}{r} v - \beta_\theta \\ \frac{\partial w}{\partial s} + \beta_s \end{Bmatrix} \quad (3)$$

where \mathbf{e} is the vector of the shell midplane strains, $\mathbf{\chi}$ is the vector of the changes in the midsurface curvatures and twist and $\mathbf{\gamma}$ is the vector of the transverse shear strains.

The constitutive relations for a laminated shell can be written as (see Appendix A):

$$\begin{Bmatrix} \bar{\mathbf{N}} \\ \bar{\mathbf{M}} \\ \bar{\mathbf{S}} \end{Bmatrix} = \begin{bmatrix} \mathbf{A} & \mathbf{B} & \mathbf{0} \\ \mathbf{B} & \mathbf{D} & \mathbf{0} \\ \mathbf{0} & \mathbf{0} & \mathbf{A}_s \end{bmatrix} \begin{Bmatrix} \boldsymbol{\varepsilon} \\ \boldsymbol{\chi} \\ \boldsymbol{\gamma} \end{Bmatrix}, \quad (4)$$

where $\bar{\mathbf{N}}$, $\bar{\mathbf{M}}$ and $\bar{\mathbf{S}}$ are vectors of the stress resultants, stress couples and shear force resultants, respectively, and \mathbf{A} , \mathbf{B} , \mathbf{D} and \mathbf{A}_s are the extensional, extensional–bending coupling, bending and transverse shear stiffness matrices, respectively, which are defined in Appendix A.

A two-node straight conical frustum element is used in this investigation; because a laminated shell exhibits in-plane extensional–shear, extensional–bending and bending–twisting couplings, its symmetric and antisymmetric modes are coupled with each other (Sheinman and Weissman, 1987). For each of the two modes, each node of the element has five independent degrees of freedom: three displacements and two rotations. Thus, the nodal displacement vector of an element may be expressed as

$$\mathbf{a} = \begin{Bmatrix} \mathbf{a}^1 \\ \mathbf{a}^2 \end{Bmatrix} \quad (5)$$

where

$$\mathbf{a}^k = [u_i^k v_i^k w_i^k \beta_{\theta i}^k \beta_{s i}^k u_j^k v_j^k w_j^k \beta_{\theta j}^k \beta_{s j}^k]^\top \quad (6)$$

in which i and j denote the front and rear ends of the frustum, respectively, and superscripts $k = 1, 2$ represent the symmetric and antisymmetric degrees of freedom, respectively.

For free vibration, the displacement field within an element for circumferential wave number, n , may be expressed as

$$[u w \beta_{\theta} \beta_s]^\top = \begin{bmatrix} \boldsymbol{\theta}_n^1 \mathbf{N} & \mathbf{0} \\ \mathbf{0} & \boldsymbol{\theta}_n^2 \mathbf{N} \end{bmatrix} \begin{Bmatrix} \mathbf{a}_n^1 \\ \mathbf{a}_n^2 \end{Bmatrix}, \quad (7)$$

where

$$\boldsymbol{\theta}_n^1 = \begin{bmatrix} \cos n\theta & 0 & 0 & 0 & 0 \\ 0 & \sin n\theta & 0 & 0 & 0 \\ 0 & 0 & \cos n\theta & 0 & 0 \\ 0 & 0 & 0 & \cos n\theta & 0 \\ 0 & 0 & 0 & 0 & \sin n\theta \end{bmatrix} \quad (8)$$

$$\boldsymbol{\theta}_n^2 = \begin{bmatrix} \sin n\theta & 0 & 0 & 0 & 0 \\ 0 & \cos n\theta & 0 & 0 & 0 \\ 0 & 0 & \sin n\theta & 0 & 0 \\ 0 & 0 & 0 & \sin n\theta & 0 \\ 0 & 0 & 0 & 0 & \cos n\theta \end{bmatrix} \quad (9)$$

$$\mathbf{N} = [N_i \mathbf{I}_3, N_j \mathbf{I}_3] \quad (10)$$

in which \mathbf{I}_5 is the 5×5 identity matrix, and N_i and N_j are the element shape functions defined as $N_i = 1 - \eta$ and $N_j = \eta$ with $\eta = s/L$. Here L is the length of the element meridian.

The Hamilton's variational principle is used here to derive the equation of motion of the shell. For the shell element considered, the potential energy Π can be written as

$$\Pi = \frac{1}{2} \int_0^{2\pi} \int_0^L (\epsilon' \bar{\mathbf{N}} + \chi' \bar{\mathbf{M}} + \gamma' \bar{\mathbf{S}}) r L d\eta d\theta \tag{11}$$

When the rotational inertia is ignored, the kinetic energy of the element T can be expressed as

$$T = \frac{1}{2} \int_0^{2\pi} \int_0^L \rho h (\dot{u}^2 + \dot{v}^2 + \dot{w}^2) r L d\eta d\theta \tag{12}$$

where h is the thickness of the shell wall and a dot represents derivative with respect to time. Applying the Hamilton's variational principle and the orthogonal property of the trigonometric functions gives the stiffness matrix for the element

$$\mathbf{K} = \int_0^L \left\{ \left[\begin{array}{cc} \bar{\mathbf{B}}_m^1 & \mathbf{0} \\ \mathbf{0} & \bar{\mathbf{B}}_m^2 \end{array} \right]^T \bar{\mathbf{A}} \left[\begin{array}{cc} \bar{\mathbf{B}}_m^1 & \mathbf{0} \\ \mathbf{0} & \bar{\mathbf{B}}_m^2 \end{array} \right] + \left[\begin{array}{cc} \bar{\mathbf{B}}_b^1 & \mathbf{0} \\ \mathbf{0} & \bar{\mathbf{B}}_b^2 \end{array} \right]^T (\bar{\mathbf{B}} + \bar{\mathbf{B}}^T) \left[\begin{array}{cc} \bar{\mathbf{B}}_b^1 & \mathbf{0} \\ \mathbf{0} & \bar{\mathbf{B}}_b^2 \end{array} \right] + \left[\begin{array}{cc} \bar{\mathbf{B}}_b^1 & \mathbf{0} \\ \mathbf{0} & \bar{\mathbf{B}}_b^2 \end{array} \right]^T \right. \\ \left. \times \bar{\mathbf{D}} \left[\begin{array}{cc} \bar{\mathbf{B}}_b^1 & \mathbf{0} \\ \mathbf{0} & \bar{\mathbf{B}}_b^2 \end{array} \right] + \left[\begin{array}{cc} \bar{\mathbf{B}}_s^1 & \mathbf{0} \\ \mathbf{0} & \bar{\mathbf{B}}_s^2 \end{array} \right]^T \bar{\mathbf{A}} \left[\begin{array}{cc} \bar{\mathbf{B}}_s^1 & \mathbf{0} \\ \mathbf{0} & \bar{\mathbf{B}}_s^2 \end{array} \right] \right\} r L d\eta \tag{13}$$

where $\bar{\mathbf{B}}_m^k = [\bar{\mathbf{B}}_{m1}^k, \bar{\mathbf{B}}_{m2}^k]$, $\bar{\mathbf{B}}_b^k = [\bar{\mathbf{B}}_{b1}^k, \bar{\mathbf{B}}_{b2}^k]$, $\bar{\mathbf{B}}_s^k = [\bar{\mathbf{B}}_{s1}^k, \bar{\mathbf{B}}_{s2}^k]$ ($k = 1, 2$) are defined in Appendix B, and adopting the notation of Sheinman and Weissman (1987):

$$\bar{\mathbf{A}} = \begin{bmatrix} A_{11} \delta_1 & A_{12} \delta_1 & 0 & 0 & 0 & A_{16} \delta_1 \\ A_{12} \delta_1 & A_{22} \delta_1 & 0 & 0 & 0 & A_{26} \delta_1 \\ 0 & 0 & A_{66} \delta_2 & A_{16} \delta_2 & A_{26} \delta_2 & 0 \\ 0 & 0 & A_{16} \delta_2 & A_{11} \delta_2 & A_{12} \delta_2 & 0 \\ 0 & 0 & A_{26} \delta_2 & A_{12} \delta_2 & A_{22} \delta_2 & 0 \\ A_{16} \delta_1 & A_{26} \delta_1 & 0 & 0 & 0 & A_{66} \delta_1 \end{bmatrix} \tag{14}$$

$\bar{\mathbf{B}}$ and $\bar{\mathbf{D}}$ are analogous to $\bar{\mathbf{A}}$, except that A_{ij} in eqn (14) is replaced by B_{ij} and D_{ij} , respectively, and

$$\bar{\mathbf{A}} = \begin{bmatrix} A_{44} \delta_2 & 0 & 0 & A_{45} \delta_1 \\ 0 & A_{33} \delta_1 & A_{13} \delta_1 & 0 \\ 0 & A_{45} \delta_2 & A_{14} \delta_1 & 0 \\ A_{45} \delta_1 & 0 & 0 & A_{33} \delta_2 \end{bmatrix} \tag{15}$$

where

$$\delta_1 = \begin{cases} 2\pi & n = 0 \\ \pi & n \neq 0 \end{cases} \quad \delta_2 = \begin{cases} 0 & n = 0 \\ \pi & n \neq 0 \end{cases}$$

In calculating the stiffness matrix from eqn (13), reduced integration should be utilized in order to avoid "shear locking" (Zienkiewicz and Taylor, 1989). One point Gauss rule is used in this paper.

Table 1. Natural frequencies (in hertz) for a clamped-free cylindrical steel shell†

n	Source	$m = 1$	$m = 2$	$m = 3$
1	Experiment (Gill, 1972)			
	Sharma (1977)			
	To and Wang (1991)	469.0	2054.0	4405.0
	This paper	468.2	2043.2	4359.0
2	Experiment (Gill, 1972)	293.0	827.0	1894.0
	Sharma (1977)	319.5	1019.7	2398.9
	To and Wang (1991)	315.7	939.1	2174.0
	This paper	312.8	926.6	2172.0
3	Experiment (Gill, 1972)	760.0	886.0	1371.0
	Sharma (1977)	769.9	930.4	1515.4
	To and Wang (1991)	766.7	909.8	1444.0
	This paper	762.8	875.7	1387.9
4	Experiment (Gill, 1972)	1451.0	1503.0	1673.0
	Sharma (1977)	1465.8	1525.0	1730.3
	To and Wang (1991)	1459.0	1501.0	1677.0
	This paper	1453.9	1466.8	1592.3
5	Experiment (Gill, 1972)	2336.0	2384.0	2480.0
	Sharma (1977)	2367.1	2409.5	2513.8
	To and Wang (1991)	2334.0	2373.0	2430.0
	This paper	2332.0	2349.6	2360.8

† $E = 210$ GPa, $G = 82$ GPa, $\nu = 0.28$, $\rho = 7800$ kg m⁻³, length = 0.502 m, radius = 0.0635 m and $h = 1.63 \times 10^{-3}$ m.

The mass matrix for the element is given by

$$\mathbf{M} = \int_0^L \rho h \begin{bmatrix} \mathbf{N}^T \mathbf{C}^1 \mathbf{N} & \mathbf{0} \\ \mathbf{0} & \mathbf{N}^T \mathbf{C}^2 \mathbf{N} \end{bmatrix} r L d\eta, \quad (16)$$

where ρ is mass density of the material and

$$\mathbf{C}^1 = \begin{bmatrix} \delta_1 & 0 & 0 & 0 & 0 \\ 0 & \delta_2 & 0 & 0 & 0 \\ 0 & 0 & \delta_3 & 0 & 0 \\ 0 & 0 & 0 & \delta_4 & 0 \\ 0 & 0 & 0 & 0 & \delta_5 \end{bmatrix}, \quad \mathbf{C}^2 = \begin{bmatrix} \delta_2 & 0 & 0 & 0 & 0 \\ 0 & \delta_1 & 0 & 0 & 0 \\ 0 & 0 & \delta_2 & 0 & 0 \\ 0 & 0 & 0 & \delta_2 & 0 \\ 0 & 0 & 0 & 0 & \delta_1 \end{bmatrix}. \quad (17)$$

For the free vibration, the eigenvalue problem is given by

$$(\mathbf{K} - \omega^2 \mathbf{M})\mathbf{a} = \mathbf{0}, \quad (18)$$

where ω is the circular frequency. For a non-trivial solution of eqn (18), the determinant of the coefficient matrix of the equation must vanish; this yields to the characteristic equation

$$|\mathbf{K} - \omega^2 \mathbf{M}| = 0. \quad (19)$$

The eigenvalues can be extracted by following the general iterative technique.

3. RESULTS AND DISCUSSION

Numerical results are obtained by using the foregoing theory. In all calculations, the shell is divided into 30 elements. Firstly, two check examples are calculated to verify the formulation and accuracy of the present analysis.

The first example is a clamped-free thin cylindrical steel shell. The clamped boundary condition implies $u = v = w = \beta_1 = \beta_0 = 0$, while at the free end all the nodal degrees of freedom are unconstrained. The natural frequencies are shown in Table 1 and compared

Table 2. Natural frequencies (in hertz) of a clamped-clamped isotropic cone†

n	m	This paper	Srinivasan and Hosur (1989)
0	1	1.094	1.092
0	2	1.382	1.375
0	3	2.069	2.044
0	4	2.630	2.630
0	5	3.030	2.993

†Length $R_2 = 1.152$, $h/R_2 = 0.08$, $\phi = 10^\circ$ and $\nu = 0.3$.

with experimental results provided by Gill (1972). This problem was studied previously by Sharma (1977) and To and Wang (1991) using semi-analytical procedures based on the Kirchhoff-Love hypothesis. Their solutions are shown in Table 1 for comparison. The agreement in these results is very good. When transverse shear deformation is considered, the shell becomes more flexible. Thus, the present results are lower than the corresponding ones in the references. When n is large and the order of longitudinal modes m is high, results given by this study and by To and Wang (1991) are slightly lower than the experimental ones. This is perhaps due to the high ratio of the transverse shear modulus to the in-plane modulus for steel.

The second example is a clamped-clamped thick isotropic cone. The natural frequencies are shown in Table 2 and compared with an integral equation solution given by Srinivasan and Hosur (1989). A good agreement is shown.

The formulation and accuracy of the present analysis are verified by these two examples. Laminated composite shells of revolution are now investigated. The material properties for the calculated shells are $E_1 = 206.9$ GPa, $E_2 = 18.62$ GPa, $G_{12} = 4.48$ GPa, $G_{13} = G_{12}$, $G_{23} = 0.5G_{12}$, $\nu_{12} = 0.28$ and $\rho = 2048$ kg m⁻³.

3.1. Thin composite cylindrical shell

A simply supported ($x=0-x$) laminated cylindrical shell is considered. At one end the boundary conditions are $u = w = \beta_x = 0$, whereas at the other end the boundary conditions are $w = \beta_x = 0$. This problem was studied previously by Sheinman and Weissman (1987) using the semi-analytical method which does not account for transverse shear deformation; because the coupling between symmetric and antisymmetric modes was discussed by Sheinman and Weissman (1987), the example is used to show the effect of transverse shear deformation.

The natural frequencies for the ($x=0-x$) shell are listed in Table 3 and compared with the results given by Sheinman and Weissman (1987). These results are for the longitudinal mode 1. It can be seen from the table that transverse shear deformation may decrease the natural frequency of the shell. This phenomenon may be explained intuitively. When transverse shear deformation is considered, the shell becomes more flexible. Thus, the present results are lower than the corresponding ones in the reference. It can be seen from the above discussion that transverse shear deformation should be included in the analysis.

3.2. Thick symmetric cross-ply cones

Figure 2 shows the variation of natural frequency with thickness to radius ratio h/R_2 for simply supported thick ($0-90^\circ$) cones. 0 and 90 layers imply the fibres run in the axial and circumferential directions, respectively. The boundary conditions are $v = w = 0$ at both ends. The results are for circumferential wave number $n = 1$ and longitudinal mode $m = 1$. It is obvious that the natural frequency increases with the thickness to radius ratio. Besides, it can also be found from the figure that the natural frequency of a thick symmetric conical shell increases with its semi-vertex angle ϕ . However, this conclusion is not valid for the thin composite cones, e.g. for $h/R_2 = 0.01$, the natural frequency of the cone with $\phi = 60^\circ$ is about 9.9% lower than that of the cone with $\phi = 45^\circ$.

Figure 3 shows the variation of natural frequency with thickness to radius ratio h/R_2 for ($0/90^\circ$), and ($90/0^\circ$), cones. The results are for circumferential wave number $n = 1$ and longitudinal mode $m = 1$. Clearly, the effect of the stacking sequence on the natural

Table 3. Natural frequencies (in hertz) of simply supported $(\alpha/0/-\alpha)$ cylindrical shells†

n	Source	α (deg)						
		0	15	30	45	60	75	90
1	Sheinman and Weissman (1987)	330.1	300.9	295.0	360.3	461.8	529.3	530.9
	This paper	328.9	297.8	286.2	341.7	443.2	515.1	519.3
2	Sheinman and Weissman (1987)	387.3	372.3	371.1	451.3	567.3	619.3	558.2
	This paper	384.8	365.9	355.6	423.7	541.1	601.9	547.8
3	Sheinman and Weissman (1987)	366.8	379.0	387.0	465.3	564.6	575.4	469.7
	This paper	364.1	371.5	368.5	435.3	539.2	561.8	463.4
4	Sheinman and Weissman (1987)	328.3	365.2	384.1	453.5	523.9	499.0	388.8
	This paper	325.7	357.1	363.2	423.4	502.7	489.6	384.7
5	Sheinman and Weissman (1987)	290.1	343.2	372.0	425.4	463.4	424.1	341.4
	This paper	287.5	334.9	349.8	398.1	447.8	417.7	338.4
6	Sheinman and Weissman (1987)	258.9	319.1	353.1	385.0	399.0	367.1	334.3
	This paper	256.2	310.6	331.2	362.7	387.7	362.1	331.9
7	Sheinman and Weissman (1987)	237.8	297.2	330.1	342.5	346.6	337.0	367.0
	This paper	234.7	288.5	309.7	324.7	337.5	332.2	364.9
8	Sheinman and Weissman (1987)	228.2	281.2	308.8	310.6	316.9	337.9	432.7
	This paper	224.7	272.3	290.3	295.0	308.0	332.4	430.7
9	Sheinman and Weissman (1987)	230.7	274.5	296.2	297.1	313.2	368.9	523.5
	This paper	226.8	265.1	278.6	281.2	303.2	361.8	521.3
10	Sheinman and Weissman (1987)	244.8	278.9	296.8	303.8	333.6	423.1	633.7
	This paper	240.6	268.9	279.0	286.4	321.8	414.9	631.1
11	Sheinman and Weissman (1987)	269.3	294.9	311.9	328.1	373.3	496.9	760.2
	This paper	264.8	284.4	293.3	309.0	359.4	486.1	757.2

†Length = 0.381 m, radius = 0.1905 m, $h = 0.501 \times 10^{-3}$ m.

frequency is profound. For $h/R_2 = 0.1$, the natural frequency of the $(0^\circ/90^\circ)_s$ cone is approximately 11.5% higher than that of the $(90^\circ/0^\circ)_s$ shell.

Figure 4 shows the variation of natural frequency with the circumferential wave number n for $(0^\circ/90^\circ)_s$ cones. The results are for longitudinal mode $m = 1$. The natural frequency of thick $(0^\circ/90^\circ)_s$ cones increases with the circumferential wave number n . The lowest natural frequency occurs at $n = 1$. It can be seen once again that the natural frequency of thick symmetric cross-ply conical shell increases with its semi-vertex angle ϕ .

3.3. Thick antisymmetric angle-ply cones

Figure 5 shows the variation of natural frequency with the ply angle α for simply supported thick $(\alpha_i/-\alpha_i/\alpha_i/-\alpha_i)$ and $(-\alpha_i/\alpha_i/-\alpha_i/\alpha_i)$ cones. The results are for circumferential wave number $n = 1$ and longitudinal mode $m = 1$. The effect of the stacking sequence on the natural frequency of the antisymmetric angle-ply cones is significant in the vicinity of $\alpha = 30^\circ$. The natural frequency of the $(30^\circ/-30^\circ/30^\circ/-30^\circ)$ cone is about 7.4% lower than

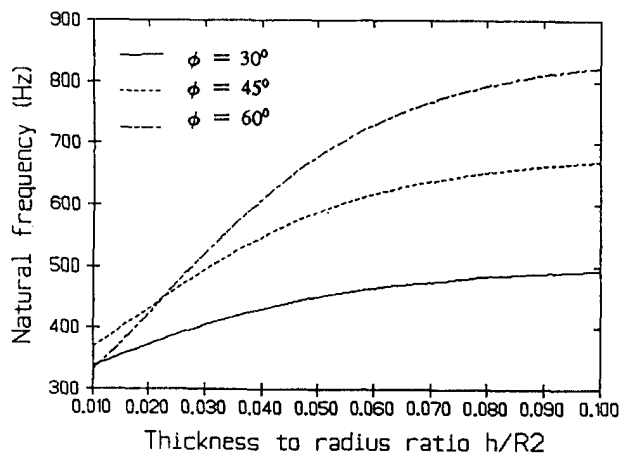


Fig. 2. Natural frequency for simply supported $(0^\circ/90^\circ)_s$ cones (length/ $R_2 = 0.5$).

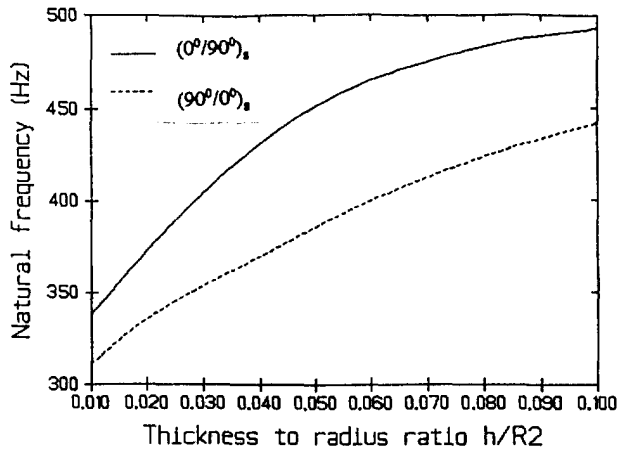


Fig. 3. Natural frequency for simply supported $(0^\circ/90^\circ)_s$ and $(90^\circ/0^\circ)_s$ cones ($\phi = 30^\circ$, length/ $R_2 = 0.5$).

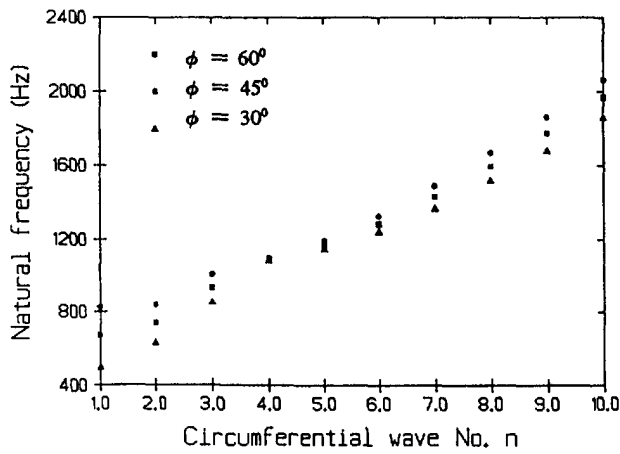


Fig. 4. Natural frequency for simply supported $(0^\circ/90^\circ)_s$ cones (length/ $R_2 = 0.5$).

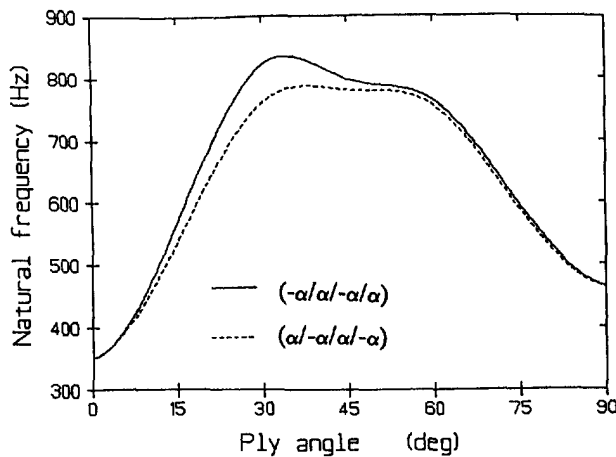


Fig. 5. Natural frequency for simply supported antisymmetric angle-ply cones ($\phi = 30^\circ$, length/ $R_2 = 0.5$).

that of the $(-30^\circ/30^\circ/-30^\circ/30^\circ)$ cone. The stacking sequence has negligible effect on the antisymmetric angle-ply cones with other values of α .

It is observed from the same figure that the ply angle may significantly affect the natural frequency of the antisymmetric angle-ply cone. The natural frequency increases to

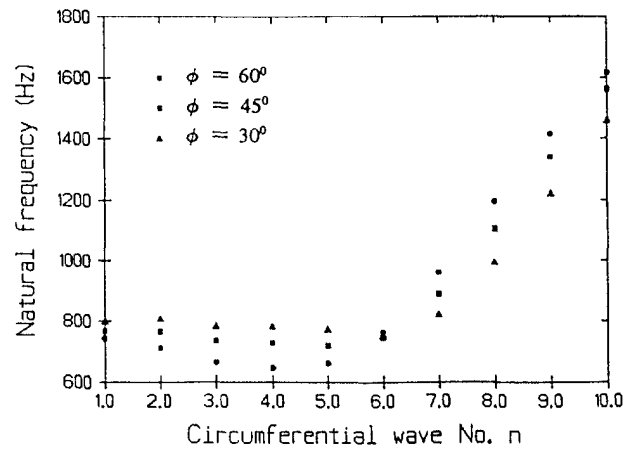


Fig. 6. Natural frequency for simply supported ($-45/45/-45/45$) cones (length $R_2 = 0.5$).

a maximum before it decreases with the ply angle. The peak values of the natural frequency for the two shells take place at $\alpha = 30^\circ$. They are 759.6 and 820.4 Hz, respectively.

Figure 6 shows the variation of the natural frequency with the circumferential wave number n for three ($-45/45/-45/45$) conical shells. The results are for longitudinal mode $m = 1$. The results in the figure indicate that the natural frequency decreases to a minimum before it increases with the number of circumferential waves. In addition, for $1 \leq n < 6$, the natural frequency of the cone decreases with its semi-vertex angle ϕ , whereas for $6 \leq n \leq 10$, the natural frequency of the cone increases with its semi-vertex angle ϕ .

4. CONCLUSIONS

The salient features of this investigation are: (1) the semi-analytical method based on the Reissner Mindlin assumption and considering the coupling between symmetric and antisymmetric modes is developed for predicting free vibration characteristics of laminated composite shells of revolution; (2) the parametric study is carried out for thin laminated composite cylindrical shells and thick symmetric cross-ply and antisymmetric angle-ply laminated composite conical shells. Based on the numerical results presented by this paper, the following conclusions may be drawn:

(1) Transverse shear deformation may reduce the natural frequency of laminated shells of revolution. Thus, the effect of shear deformation should be included in the analysis.

(2) The effect of the stacking sequence on the natural frequency of a thick symmetric cross-ply cone is profound. The natural frequency of a symmetric cross-ply cone increases with the circumferential wave number, the semi-vertex angle and the thickness to radius ratio.

(3) The ply angle may significantly affect the natural frequency of a thick antisymmetric angle-ply cone. The ($30/-30/30/-30$) and ($-30/30/-30/30$) cones have higher natural frequency. Although the effect of stacking sequence is strong for $\alpha = 30^\circ$, it is negligible for the antisymmetric angle-ply cones with other values of α . The natural frequency of an antisymmetric angle-ply cone first decreases and then increases with its semi-vertex angle and the number of circumferential waves.

Acknowledgement— The authors are grateful to the Research Committee of The Hong Kong Polytechnic University for the financial support of this investigation.

REFERENCES

- Bert, C. W. and Kumar, M. (1982). Vibration of cylindrical shell of bimodulus composite materials. *J. Sound Vib.* **81**, 107–121.

Bismarck-Nasr, M. N. (1992). Finite element analysis of aeroelasticity of plates and shells. *Appl. Mech. Rev.* **45**, 463-482.

Cook, R. D. (1981). *Concepts and Applications of Finite Element Analysis*, 3rd Edn. John Wiley, New York.

Gallagher, R. H. (1975). Shell elements. In *World Conference on Finite Element Methods in Structural Mechanics*. Bournemouth, Dorset, England.

Gill, P. A. T. (1972). Vibrations of clamped-free circular cylindrical shells. *J. Sound Vibr.* **25**, 501-503.

Grafton, P. E. and Strome, D. R. (1963). Analysis of axi-symmetric shells by the direct stiffness method. *AIAA J.* **1**, 2342-2347.

Noor, A. K. and Burton, W. S. (1990). Assessment of computational models for multilayered composite shells. *Appl. Mech. Rev.* **43**, 67-97.

Sharma, C. B. (1977). Simple linear formulas for critical frequencies for cantilever circular cylindrical shells. *J. Sound Vibr.* **55**, 467-471.

Sheinman, I. and Grief, S. (1984). Dynamic analysis of laminated shells of revolution. *J. Compos. Mater.* **18**, 200-215.

Sheinman, I. and Weissman, S. (1987). Coupling between symmetric and antisymmetric modes in shells of revolution. *J. Compos. Mater.* **21**, 988-1007.

Shivakumar, K. N. and Krishnamurthy, A. V. (1978). A high precision ring element for vibration of laminated shells. *J. Sound Vibr.* **58**, 311-318.

Sivadas, K. R. and Ganesan, N. (1992). Vibration analysis of orthotropic cantilever cylindrical shells with axial thickness variation. *Compos. Structures* **22**, 207-215.

Srinivasan, R. S. and Hosur, V. (1989). Axisymmetric vibration of thick conical shells. *J. Sound Vibr.* **135**, 171-176.

To, C. W. S. and Wang, B. (1991). An axisymmetric thin shell finite element for vibration analysis. *Comput. Structures* **40**, 555-568.

Tsai, S. W. and Hahn, H. T. (1980). *Introduction to Composite Materials*. Technomic Publishing, Westport, Connecticut.

Zienkiewicz, O. C., Bauer, J., Morgan, K. and Onate, E. (1977). A simple and efficient element for axisymmetric shells. *Int. J. Numer. Meth. Engng* **11**, 1545-1558.

Zienkiewicz, O. C. and Taylor, R. L. (1989). *The finite element method*, 4th edn. McGraw-Hill, London.

APPENDIX A: CONSTITUTIVE RELATIONS FOR THE LAMINATE

In a ply coordinate system 1-2-3 (see Fig. A1), the stress-strain relations for any ply are given by (Tsai and Hahn, 1980):

$$\begin{Bmatrix} \sigma_1 \\ \sigma_2 \\ \tau_{12} \\ \sigma_3 \\ \sigma_4 \\ \sigma_5 \end{Bmatrix} = \begin{bmatrix} Q_{11} & Q_{12} & 0 & 0 & 0 \\ Q_{12} & Q_{22} & 0 & 0 & 0 \\ 0 & 0 & Q_{66} & 0 & 0 \\ 0 & 0 & 0 & Q_{44} & 0 \\ 0 & 0 & 0 & 0 & Q_{55} \end{bmatrix} \begin{Bmatrix} \epsilon_1 \\ \epsilon_2 \\ \gamma_{12} \\ \epsilon_3 \\ \epsilon_4 \\ \epsilon_5 \end{Bmatrix} \quad (A1)$$

where Q_{ij} ($i, j = 1, 2, 4, 5, 6$) are the reduced stiffnesses of a ply and are related to material properties of a ply as follows:

$$Q_{11} = \frac{E_1}{1 - \nu_{12}\nu_{21}}, \quad Q_{22} = \frac{\nu_{12}E_1}{1 - \nu_{12}\nu_{21}}, \quad Q_{33} = \frac{E_3}{1 - \nu_{13}\nu_{31}}, \quad Q_{44} = G_{44}, \quad Q_{55} = G_{55}, \quad (A2)$$

On transformation, the stress-strain relations in terms of global coordinates are obtained as:

$$\begin{Bmatrix} \sigma_x \\ \sigma_y \\ \tau_{xy} \\ \tau_x \\ \tau_y \end{Bmatrix} = \begin{bmatrix} \bar{Q}_{11} & \bar{Q}_{12} & \bar{Q}_{13} & 0 & 0 \\ \bar{Q}_{12} & \bar{Q}_{22} & \bar{Q}_{23} & 0 & 0 \\ \bar{Q}_{13} & \bar{Q}_{23} & \bar{Q}_{33} & 0 & 0 \\ 0 & 0 & 0 & \bar{Q}_{44} & \bar{Q}_{45} \\ 0 & 0 & 0 & \bar{Q}_{45} & \bar{Q}_{55} \end{bmatrix} \begin{Bmatrix} \epsilon_x \\ \epsilon_y \\ \gamma_{xy} \\ \gamma^x \\ \gamma^y \end{Bmatrix} \quad (A3)$$

where \bar{Q}_{ij} ($i, j = 1, 2, 4, 5, 6$) are the transformed reduced stiffnesses of any ply and are related to Q_{ij} as follows:

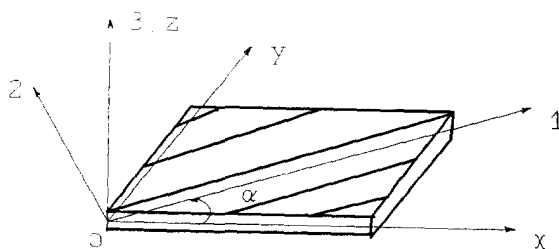


Fig. A1. Ply and global coordinates.

$$\begin{aligned}
\bar{Q}_{11} &= U_1 + U_2 \cos 2\alpha + U_3 \cos 4\alpha \\
\bar{Q}_{12} &= U_4 - U_3 \cos 4\alpha \\
\bar{Q}_{16} &= \frac{1}{2} U_2 \sin 2\alpha + U_3 \sin 4\alpha \\
\bar{Q}_{22} &= U_1 - U_2 \cos 2\alpha + U_3 \cos 4\alpha \\
\bar{Q}_{26} &= \frac{1}{2} U_2 \sin 2\alpha - U_3 \sin 4\alpha \\
\bar{Q}_{66} &= U_5 - U_3 \cos 4\alpha \\
\bar{Q}_{44} &= Q_{55} \sin^2 \alpha + Q_{44} \cos^2 \alpha \\
\bar{Q}_{45} &= (Q_{55} - Q_{44}) \sin \alpha \cos \alpha \\
\bar{Q}_{55} &= Q_{55} \cos^2 \alpha + Q_{44} \sin^2 \alpha
\end{aligned} \tag{A4}$$

with α being ply angle and

$$\begin{aligned}
U_1 &= \frac{1}{8}(3Q_{11} + 3Q_{22} + 2Q_{12} + 4Q_{66}), \quad U_2 = \frac{1}{2}(Q_{11} - Q_{22}) \\
U_3 &= \frac{1}{8}(Q_{11} + Q_{22} - 2Q_{12} - 4Q_{66}), \quad U_4 = \frac{1}{8}(Q_{11} + Q_{22} + 6Q_{12} - 4Q_{66}) \\
U_5 &= \frac{1}{8}(Q_{11} + Q_{22} - 2Q_{12} + 4Q_{66}).
\end{aligned} \tag{A5}$$

The constitutive relations for laminated shells can be obtained by integrating the stresses and stresses multiplied by the coordinate z through the thickness of the shell as follows:

$$\bar{\mathbf{N}} = \begin{Bmatrix} N_x \\ N_\theta \\ N_{\phi\phi} \end{Bmatrix} = \begin{bmatrix} A_{11} & A_{12} & A_{16} \\ A_{12} & A_{22} & A_{26} \\ A_{16} & A_{26} & A_{66} \end{bmatrix} \begin{Bmatrix} \varepsilon_x \\ \varepsilon_\theta \\ \gamma_{\phi\theta} \end{Bmatrix} + \begin{bmatrix} B_{11} & B_{12} & B_{16} \\ B_{12} & B_{22} & B_{26} \\ B_{16} & B_{26} & B_{66} \end{bmatrix} \begin{Bmatrix} \chi_x \\ \chi_\theta \\ \chi_{\phi\theta} \end{Bmatrix} \tag{A6}$$

$$\bar{\mathbf{M}} = \begin{Bmatrix} M_x \\ M_\theta \\ M_{\phi\phi} \end{Bmatrix} = \begin{bmatrix} B_{11} & B_{12} & B_{16} \\ B_{12} & B_{22} & B_{26} \\ B_{16} & B_{26} & B_{66} \end{bmatrix} \begin{Bmatrix} \varepsilon_x \\ \varepsilon_\theta \\ \gamma_{\phi\theta} \end{Bmatrix} + \begin{bmatrix} D_{11} & D_{12} & D_{16} \\ D_{12} & D_{22} & D_{26} \\ D_{16} & D_{26} & D_{66} \end{bmatrix} \begin{Bmatrix} \chi_x \\ \chi_\theta \\ \chi_{\phi\theta} \end{Bmatrix} \tag{A7}$$

$$\mathbf{S} = \begin{Bmatrix} S_n \\ S_s \end{Bmatrix} = \begin{bmatrix} A_{44} & A_{45} \\ A_{45} & A_{55} \end{bmatrix} \begin{Bmatrix} \gamma_{\theta z} \\ \gamma_{xz} \end{Bmatrix} \tag{A8}$$

Equations (A6)–(A8) can be simplified as

$$\begin{Bmatrix} \bar{\mathbf{N}} \\ \bar{\mathbf{M}} \\ \mathbf{S} \end{Bmatrix} = \begin{bmatrix} \mathbf{A} & \mathbf{B} & \mathbf{0} \\ \mathbf{B} & \mathbf{D} & \mathbf{0} \\ \mathbf{0} & \mathbf{0} & \mathbf{A}_s \end{bmatrix} \begin{Bmatrix} \boldsymbol{\varepsilon} \\ \boldsymbol{\chi} \\ \boldsymbol{\gamma} \end{Bmatrix} \tag{A9}$$

where $\bar{\mathbf{N}}$, $\bar{\mathbf{M}}$ and \mathbf{S} are vectors of the stress resultants, stress couples and shear force resultants, respectively, and \mathbf{A} , \mathbf{B} , \mathbf{D} and \mathbf{A}_s are the extensional, extensional-bending coupling, bending and transverse shear stiffness matrices, respectively, defined by

$$\begin{aligned}
(A_{ij}, B_{ij}, D_{ij}) &= \int_{-h/2}^{h/2} \bar{Q}_{ij}(1, z, z^2) dz \quad (i, j = 1, 2, 6) \\
A_{\phi\theta} &= \frac{5}{4} \int_{-h/2}^{h/2} \bar{Q}_{\phi\theta} \left(1 - \frac{4z^2}{h^2}\right) dz \quad (i, j = 4, 5),
\end{aligned} \tag{A10}$$

with h being thickness of the shell wall.

APPENDIX B: STRAIN-DISPLACEMENT MATRICES

$$\bar{\mathbf{B}}_{mr}^1 = \begin{bmatrix} -1/r & 0 & 0 & 0 & 0 \\ (1-\eta) \sin \phi/r & n(1-\eta)/r & (1-\eta) \cos \phi/r & 0 & 0 \\ -n(1-\eta)/r & [-1/L - (1-\eta) \sin \phi/r] & 0 & 0 & 0 \end{bmatrix} \tag{B1}$$

$$\bar{\mathbf{B}}_{mr}^1 = \begin{bmatrix} 1/L & 0 & 0 & 0 & 0 \\ \eta \sin \phi/r & n\eta/r & \eta \cos \phi/r & 0 & 0 \\ -n\eta/r & (1/L - \eta \sin \phi/r) & 0 & 0 & 0 \end{bmatrix} \tag{B2}$$

$$\bar{\mathbf{B}}_{bt}^1 = \begin{bmatrix} 0 & 0 & 0 & 1/L & 0 \\ 0 & 0 & 0 & -(1-\eta)\sin\phi/r & -n(1-\eta)/r \\ n(1-\eta)\cos\phi/2r^2 & [-\cos\phi/2rL + (1-\eta)\sin 2\phi/4r^2] & 0 & n(1-\eta)/r & [(1-\eta)\sin\phi/r + 1/L] \end{bmatrix} \quad (\text{B3})$$

$$\bar{\mathbf{B}}_{bt}^2 = \begin{bmatrix} 0 & 0 & 0 & -1/L & 0 \\ 0 & 0 & 0 & -\eta\sin\phi/r & -n\eta/r \\ n\eta\cos\phi/2r^2 & (\cos\phi/2rL + \eta\sin 2\phi/4r^2) & 0 & n\eta/r & (\eta\sin\phi/r - 1/L) \end{bmatrix} \quad (\text{B4})$$

$$\bar{\mathbf{B}}_{st}^1 = \begin{bmatrix} 0 & -(1-\eta)\cos\phi/r & -n(1-\eta)/r & 0 & -(1-\eta) \\ 0 & 0 & -1/L & (1-\eta) & 0 \end{bmatrix} \quad (\text{B5})$$

$$\bar{\mathbf{B}}_{st}^2 = \begin{bmatrix} 0 & -\eta\cos\phi/r & -n\eta/r & 0 & -\eta \\ 0 & 0 & 1/L & \eta & 0 \end{bmatrix} \quad (\text{B6})$$

$$\bar{\mathbf{B}}_{mz}^2 = \begin{bmatrix} -1/L & 0 & 0 & 0 & 0 \\ (1-\eta)\sin\phi/r & -n(1-\eta)/r & (1-\eta)\cos\phi/r & 0 & 0 \\ n(1-\eta)/r & (-1/L - (1-\eta)\sin\phi/r) & 0 & 0 & 0 \end{bmatrix} \quad (\text{B7})$$

$$\bar{\mathbf{B}}_{mz}^1 = \begin{bmatrix} 1/L & 0 & 0 & 0 & 0 \\ \eta\sin\phi/r & -n\eta/r & \eta\cos\phi/r & 0 & 0 \\ n\eta/r & (1/L - \eta\sin\phi/r) & 0 & 0 & 0 \end{bmatrix} \quad (\text{B8})$$

$$\bar{\mathbf{B}}_{bz}^2 = \begin{bmatrix} 0 & 0 & 0 & 1/L & 0 \\ 0 & 0 & 0 & -(1-\eta)\sin\phi/r & n(1-\eta)/r \\ -n(1-\eta)\cos\phi/2r^2 & [-\cos\phi/2rL + (1-\eta)\sin 2\phi/4r^2] & 0 & -n(1-\eta)/r & [(1-\eta)\sin\phi/r + 1/L] \end{bmatrix} \quad (\text{B9})$$

$$\bar{\mathbf{B}}_{bz}^1 = \begin{bmatrix} 0 & 0 & 0 & -1/L & 0 \\ 0 & 0 & 0 & -\eta\sin\phi/r & n\eta/r \\ -n\eta\cos\phi/2r^2 & (\cos\phi/2rL + \eta\sin 2\phi/4r^2) & 0 & -n\eta/r & (\eta\sin\phi/r - 1/L) \end{bmatrix} \quad (\text{B10})$$

$$\bar{\mathbf{B}}_{sz}^2 = \begin{bmatrix} 0 & -(1-\eta)\cos\phi/r & n(1-\eta)/r & 0 & -(1-\eta) \\ 0 & 0 & -1/L & (1-\eta) & 0 \end{bmatrix} \quad (\text{B11})$$

$$\bar{\mathbf{B}}_{sz}^1 = \begin{bmatrix} 0 & -\eta\cos\phi/r & n\eta/r & 0 & -\eta \\ 0 & 0 & 1/L & \eta & 0 \end{bmatrix} \quad (\text{B12})$$

Here $r = r_s + (r_l - r_s)\eta$ where r_s and r_l indicate the radius of the element at its small and large ends, respectively.